Hall effect study of the κ -(ET) 2X family : Evidence for Mott-Anderson localization

Čulo, Matija; Tafra, Emil; Mihaljević, Bojan; Basletić, Mario; Kuveždić, Marko; Ivek, Tomislav; Hamzić, Amir; Tomić, Silvia; Hiramatsu, T.; Yoshida, Y.; ...

Source / Izvornik: **Physical Review B, 2019, 99**

Journal article, Published version
Rad u časopisu, Objavljena verzija rada (izdavačev PDF)

https://doi.org/10.1103/physrevb.99.045114

Permanent link / Trajna poveznica: https://urn.nsk.hr/urn:nbn:hr:217:756852

Editors' Suggestion

Hall effect study of the κ-$(ET)_2X$ family: Evidence for Mott-Anderson localization

M. Čulo,[1,*] E. Tafra,[2] B. Mihaljević,[2] M. Basletić,[2] M. Kuveždić,[2] T. Ivek,[1] A. Hamzić,[2] S. Tomić,[1] T. Hiramatsu,[3] Y. Yoshida,[3,4] G. Saito,[3,5] J. A. Schlueter,[6,7] M. Dressel,[8] and B. Korin-Hamzić[1]

[1]*Institut za fiziku, P.O. Box 304, HR-10001 Zagreb, Croatia*

[2]*Department of Physics, Faculty of Science, University of Zagreb, Bijenička cesta 32, HR-10000 Zagreb, Croatia*

[3]*Faculty of Agriculture, Meijo University, 1-501 Shiogamaguchi, Tempaku-ku, Nagoya 468-8502, Japan*

[4]*Division of Chemistry, Graduate School of Science, Kyoto University, Sakyo-ku, Kyoto 606-8502, Japan*

[5]*Toyota Physical and Chemical Research Institute, Nagakute 480-1192, Japan*

[6]*Division of Materials Research, National Science Foundation, 2415 Eisenhower Avenue, Alexandria, Virginia 22314, USA*

[7]*Material Science Division, Argonne National Laboratory, Argonne, Illinois 60439-4831, USA*

[8]*1. Physikalisches Institut, Universität Stuttgart, Pfaffenwaldring 57, D-70550 Stuttgart, Germany*

(Received 15 October 2018; revised manuscript received 13 December 2018; published 8 January 2019)

We investigate the dc resistivity and Hall effect of the quasi-two-dimensional organic materials κ-$(ET)_2X$, where $X = Ag_2(CN)_3$ and $B(CN)_4$ and compare them with the results for $X = Cu_2(CN)_3$. All three compounds are considered to be quantum-spin-disordered Mott insulators. Despite high similarities in chemical composition and crystal structure, large differences in the dc resistivity and Hall coefficient are found. While around room temperature the dc transport properties are dominantly determined by the strength of the electron correlations, upon reducing the temperature, dc transport happens by hopping due to inherent disorder. The most disordered compound with $X = Cu_2(CN)_3$ turns out to have the lowest dc resistivity and the highest charge carrier density, i.e., in the phase diagram it is located closest to the metal-insulator transition. The least disordered compound with $X = B(CN)_4$ shows the highest resistivity and the lowest carrier density, i.e., lies farthest from the metal-insulator transition. We explain such counterintuitive behavior within the theory of Mott-Anderson localization as a consequence of disorder-induced localized states within the correlation gap.

DOI: 10.1103/PhysRevB.99.045114

I. INTRODUCTION

The family of compounds based on the bis(ethylenedithio)tetrathiafulvalene (BEDT-TTF or ET for short) molecule is considered as one of the most prominent model systems for studying electron correlations in two dimensions. The history started in the early 1980's with the realization of many interesting two-dimensional (2D) compounds following the successful synthesis of the ET molecule [1]. This family has been intensively investigated because of unconventional superconductivity which bears some similarities to the superconductivity in cuprates [2]. Besides that, the ET family shows various other exotic phenomena such as charge ordering, ferroelectricity, Dirac fermions, Mott transition, quantum spin liquid, etc.

The ET family has a layered crystal structure which consists of organic ET layers and inorganic X layers alternately stacked one on another, where X represents various inorganic anions. Because of charge transfer between ET and X layers (two ET molecules donate one electron to an inorganic formula unit X on average), organic layers become conducting and inorganic layers become insulating. Since charges move much more easily inside conductive layers than perpendicular to them, the ET family shows quasi-2D electronic properties. Except for the inorganic anion X, the physical properties of various members of the family depend also on the arrangement of the ET molecules inside the conducting layers denoted by Greek letters such as α, β, κ, and θ.

Here, we focus on the κ-type arrangement where ET molecules inside organic layers are paired in dimers which form a triangular lattice so that each dimer is oriented approximately perpendicular to its neighbors. Since according to the charge transfer there is one hole per dimer, the majority of theoretical models are based on a half-filled Hubbard Hamiltonian on an anisotropic triangular lattice [2]. The model is based on two transfer integrals between neighboring dimers t and t' and the effective Coulomb repulsion between two electrons on the same dimer U. Depending on the correlation strength which is usually defined as U/W, where W is the bandwidth, a system is in the Mott insulating state (large U/W) or in the metallic state (small U/W). In the Mott insulating state the Hubbard Hamiltonian can be transformed to the Heisenberg Hamiltonian which describes spin degrees of freedom and which is on the anisotropic triangular lattice defined by the superexchange antiferromagnetic interactions $J = -2t^2/U$ and $J' = -2t'^2/U$ [2]. Therefore, it is expected that the ground state of a Mott insulator is antiferromagnetic.

The correlation strength U/W can be varied experimentally either by hydrostatic pressure or by studying materials with different inorganic anions X. Recently, we have studied [3,4] the material κ-$(ET)_2Cu_2(CN)_3$ which has an

*mculo@ifs.hr; present address: High Field Magnet Laboratory (HFML-EMFL), Institute for Molecules and Materials, Radboud University, Toernooiveld 7, 6525 ED, Nijmegen, Netherlands.

intermediate correlation strength $U/W \approx 1$ [5–8], and which is, according to the phase diagram, a Mott insulator close to a boundary with the metallic state. Based on early studies it belongs to the monoclinic system with the space group $P2_1/c$ and with four ET molecules per unit cell [5,9]. However, a most recent in-depth investigation revealed a triclinic symmetry structure with the $P\bar{1}$ space group [10]. Crystallographic b and c axes are within the conducting ET layers while the crystallographic a^* axis is perpendicular to them. Despite a strong antiferromagnetic superexchange interaction $J \approx 250$ K, no long-range magnetic order has been detected down to temperatures as low as 30 mK [11]. κ-$(ET)_2Cu_2(CN)_3$ is therefore considered as one of the first realizations of the quantum spin-liquid state theoretically proposed by Anderson [12] more than 40 years ago. The absence of long-range magnetic order is commonly ascribed to the geometric frustration on an almost isotropic triangular lattice. Namely, the ratio of the interdimer transfer integrals in κ-$(ET)_2Cu_2(CN)_3$, $t'/t \approx 0.83$, is very close to unity [5,6,13], so it is impossible to arrange all spins in such a way to fulfill both antiferromagnetic superexchange interactions J and J'.

A dc transport study [3] of κ-$(ET)_2Cu_2(CN)_3$ showed the absence of a well-defined correlation (Mott-Hubbard) gap, expected for Mott insulators [14], in accordance with optical conductivity measurements [15]. The study indicated that charge transport at low temperatures takes place via Mott 2D variable-range hopping (VRH), which was later confirmed by magnetotransport measurements [4]. Such behavior, together with a relaxorlike dielectric response [3,16], implied the presence of disorder within the conducting ET layers, which was somewhat surprising since the corresponding single crystals were nominally clean. However, it is known that in the case of κ-$(ET)_2Cu_2(CN)_3$, some CN groups lie on inversion centers and are therefore crystallographically disordered [5]. It was suggested [3] that this intrinsic disorder within insulating $Cu_2(CN)_3$ layers is transferred to conducting ET layers via hydrogen bonds between ethylene groups of the ET molecules and the disordered CN groups. There is now a growing body of evidence that this charged disorder, besides the geometric frustration, plays an important role in the formation of the quantum spin-liquid ground state [17–19].

The presence of hopping conductivity indicates that κ-$(ET)_2Cu_2(CN)_3$ cannot be considered as a simple Mott insulator, the insulating properties of which stem from the existence of a correlation gap. In fact, κ-$(ET)_2Cu_2(CN)_3$ is more similar to Anderson insulators which are gapless but have disorder-induced localized states at the Fermi level giving rise to hopping conductivity. It was therefore suggested [3] that the properties of κ-$(ET)_2Cu_2(CN)_3$ should be considered within the more advanced theory of Mott-Anderson localization.

There are several theoretical studies of the Mott-Anderson localization [20–22] which are in principle based on two parameters: a correlation strength U/W and a disorder strength Δ. According to theory, a simple Mott insulator with a well-defined correlation gap exists only in the case when there is no disorder, i.e., $\Delta = 0$. Similarly, a simple gapless Anderson insulator exists only when there are no correlations, i.e., $U/W = 0$. When there are both correlations and disorder, the energy spectrum is in general quite complicated and consists of localized and delocalized states so that a distinction mentioned earlier is no longer possible.

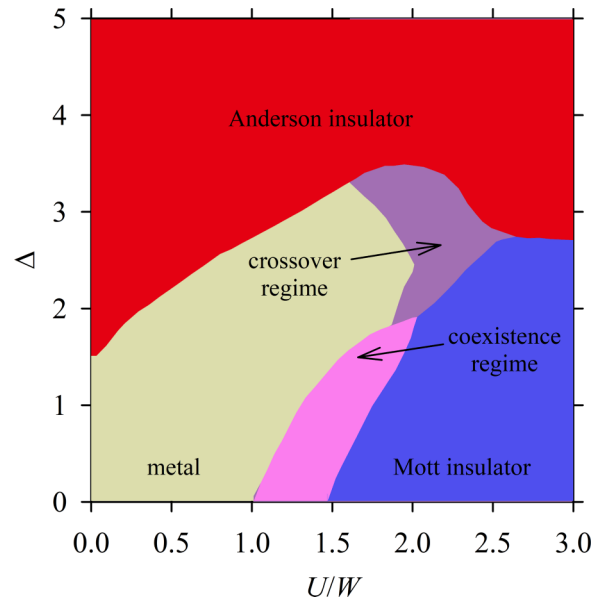

FIG. 1. A sketch of the Mott-Anderson phase diagram. This figure is based on data from Ref. [20].

The main results of the Mott-Anderson localization theory [20–22] are summarized in a phase diagram spanned by U/W and Δ axes (see Fig. 1). In the limit of low U/W, increasing disorder drives a system from a metallic to an Anderson insulating state. Such behavior is qualitatively similar to the one found in conventional Anderson insulators. In the opposite limit of high U/W, increasing disorder pushes the system from the Mott insulating directly to the Anderson insulating state. In the most complicated part of the phase diagram with intermediate U/W, there is a Mott insulating state for small Δ, an Anderson insulating state for large Δ, and a metallic state for intermediate Δ. Besides that, there is also a regime of coexistence between the Mott insulating and metallic state and a crossover regime between the Mott insulating and Anderson insulating state. Therefore, to study the theory of Mott-Anderson localization it is desirable to tune the correlation U/W and/or the disorder strength Δ.

Here, we report a detailed dc resistivity and Hall effect study of the two important members of the κ-$(ET)_2X$ family, κ-$(ET)_2Ag_2(CN)_3$ and κ-$(ET)_2B(CN)_4$, and compare them with our previous results for κ-$(ET)_2Cu_2(CN)_3$ [3,4]. From now on we will refer to the three compounds simply as κ-Cu, κ-Ag, and κ-B, respectively.

κ-Ag has the same crystal structure as κ-Cu with the correlation strength $U/W \approx 1$, [7,8] and frustration strength $t'/t \approx 0.97$ [23], which are close to the ones found in κ-Cu. Accordingly, κ-Ag is also a Mott insulator with a quantum spin-liquid ground state [23]. Previous dc resistivity and dielectric spectroscopy measurements published by our group [24] revealed the presence of 2D VRH at low temperatures and relaxorlike behavior which were both ascribed to the CN disorder within insulating $Ag_2(CN)_3$ layers transferred to conducting layers via hydrogen bonds between ethylene and disordered CN groups, in full analogy with κ-Cu [3].

However, the degree of disorder within the conducting ET layers in κ-Ag is lower than in κ-Cu due to longer contacts between the disordered CN groups and terminal ethylene groups of ET molecules [7,24].

The crystal structure of κ-B is orthorhombic with space group *Pnma* and with eight ET molecules per unit cell. ET layers are parallel to crystallographic *ac* planes while the crystallographic *b* axis is perpendicular to them. The correlation strength $U/W \approx 1$ [25–27], as the one in κ-Cu and κ-Ag. Here, it is important to mention that U/W values can differ even by a factor of 2 depending on the calculation method, either extended Hückel [7] or first-principles density functional theory calculations [5,6,25]. The latter calculations do not exist for κ-Ag while extended Hückel calculations give values for U/W at 300 K: 0.929, 1.043, and 1.1 for κ-Cu, κ-Ag, and κ-B, respectively [7]. The frustration strength $t'/t \approx 1.44$ is significantly larger than in κ-Cu and κ-Ag, indicating a more pronounced quasi-1D nature of κ-B in accordance with magnetic susceptibility measurements [25]. Similar to κ-Cu and κ-Ag, no long-range antiferromagnetic order has been detected down to the lowest measured temperatures despite a strong antiferromagnetic superexchange interaction. However, κ-B has a spin-gapped nonmagnetic ground state [25], unlike κ-Cu and κ-Ag for which it is suggested to form a quantum spin-liquid state.

The $B(CN)_4$ anion is orientationally ordered already at room temperature so there are no crystallographically disordered CN groups [25]. That means that κ-B is the most ordered of the three compounds, i.e., going from κ-Cu, across κ-Ag, to κ-B, the disorder strength Δ decreases. This is convenient, because it enables us to consider some ideas within the Mott-Anderson localization theory and apply them to the selected three materials. In this paper we show that despite the apparently similar values of correlation strengths U/W, there are large differences in dc resistivity and Hall effect between κ-Cu, κ-Ag, and κ-B which can be ascribed to different levels of disorder within the conducting ET layers. The most disordered κ-Cu turns out to have the lowest resistivity normalized to the room-temperature value and the highest charge carrier density, i.e., lies closest to the metal-insulator transition. On the other hand, the least disordered κ-B has the highest normalized resistivity and the lowest carrier density so it is farthest from the metal-insulator transition. We find that such behavior is consistent with the theory of Mott-Anderson localization according to which for low Δ increasing disorder causes the appearance of localized states within a correlation gap, leading in turn to higher conductivity and higher carrier density.

II. SAMPLES AND METHODS

Single crystals of κ-Ag and κ-B were produced by galvanostatic oxidation of ET molecules [7,25]. In contrast to single crystals of κ-Cu, which were thin plates of a rectangular shape [3], single crystals of κ-Ag and κ-B are quite thick and have an elongated hexagonal or squarelike shape. The typical dimensions are $0.7 \times 0.5 \times 0.2\ mm^3$ for the hexagonal samples and $0.5 \times 0.5 \times 0.2\ mm^3$ for the square ones. The samples were oriented on the basis of x-ray backreflection Laue photographs done after dc resistivity and Hall effect

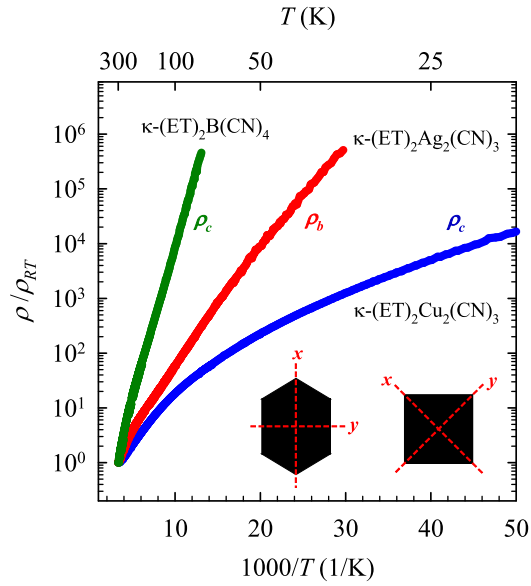

FIG. 2. Temperature dependence of the dc resistivity normalized to the room-temperature ρ/ρ_{RT} along the highest-conducting direction for κ-Cu (*c* direction, blue line), κ-Ag (*b* direction, red line), and κ-B (*c* direction, green line). Inset: In-plane crystallographic directions for hexagonal and squarelike samples (*x* and *y* in the case of κ-Ag correspond to the crystallographic *b* and *c* axis and in the case of κ-B to the *a* and *c* axis, respectively).

experiments. The largest surface of the samples is parallel to the 2D ET layers which in the case of κ-Cu and κ-Ag corresponds to crystallographic *bc* planes, while in the case of κ-B it corresponds to crystallographic *ac* planes. Crystallographic a^* and *b* axes are perpendicular to the *bc* and *ac* planes, respectively. While the in-plane directions in the case of κ-Cu were parallel to the edges of the sample surface, the situation for the κ-Ag and κ-B samples is more complicated since the in-plane directions are not directed along the edges of the sample surface but near the sample diagonals (see the inset of Fig. 2).

Contacts for the dc resistivity and Hall effect measurements were made by applying conductive carbon paint directly to the sample surface. The dc resistivity was measured by a standard four-contact technique in the temperature interval $30\ K < T < 300\ K$ along all three principal directions. The Hall coefficient R_H was measured in the temperature range $100\ K < T < 300\ K$, and in magnetic fields *B* up to 9 T. For all samples, the current *I* was applied along the highest-conducting direction and the magnetic field was oriented along the lowest-conducting direction, i.e., perpendicular to conducting ET planes as in κ-Cu [3]. The measurements were performed at fixed temperatures and in field sweeps from $-B_{max}$ to $+B_{max}$. The Hall voltage was determined as $V_{xy} = [V_{xy}(+B) - V_{xy}(-B)]/2$ in order to eliminate the possible mixing of the magnetoresistance component. The Hall resistance $R_{xy} = V_{xy}/I$ was linear with the magnetic field in the whole temperature interval investigated for all samples and the Hall coefficient was obtained as $R_H = V_{xy}w/(IB)$, where *w* is the sample thickness. The magnetoresistance of κ-Ag and κ-B was below the resolution of our experiment in the entire temperature range.

Contacts for the dc in-plane and out-of plane resistivity as well as the Hall effect measurements were arranged as in our previous work on κ-Cu [3]. Accordingly, in the case of the in-plane resistivity and Hall effect measurements, the contacts were placed on the lateral sides of the plates so that the current flows through the whole thickness of the sample. For some of the κ-Ag and κ-B samples, especially the thicker ones, such an arrangement of the contacts caused a very inhomogeneous current flow through the sample. It is known that inhomogeneous current flow can appear in the case of a bad sample geometry and can strongly influence the Hall effect measurements [28,29]. Here, a significant reduction of the inhomogeneity of the current flow was achieved by placing all contacts on the surface of the plates. Since for such an arrangement the current does not flow through the whole thickness of the sample, the measured resistivity is larger than the actual in-plane resistivity. However, it was shown [30,31] that if a sample satisfies the relation $w/l \geqslant (\rho_{\parallel}/\rho_{zz})^{1/2}$, which is always fulfilled for our samples, the actual in-plane resistivity $\rho_{\parallel}$ can be calculated from the measured resistivity ρ_m using the expression

$$\rho_m \approx 2(w/l)(\rho_{\parallel}\rho_{zz})^{1/2}, \tag{1}$$

where w is the sample thickness, l is a distance between the current contacts, ρ_{zz} is the out-of-plane resistivity, $\rho_{\parallel} \approx 1/2(\rho_{xx} + \rho_{yy})$, and ρ_{xx} and ρ_{yy} are the two in-plane resistivities. Knowing the actual in-plane resistivity we were able to calculate the effective thickness of the sample that participates in conduction which was necessary for the Hall effect data analysis.

III. RESULTS AND DISCUSSION

A. Hopping conductivity and disorder within insulating layers

Figure 2 presents the temperature dependence of the dc resistivity ρ along the highest-conducting direction for all three compounds κ-Cu, κ-Ag, and κ-B. The results confirm our previous data [4,24,25]. The average room-temperature resistivity values ρ_{RT} are 70, 450, and 260 mΩ cm for κ-Cu, κ-Ag, and κ-B, respectively. In order to highlight the difference in temperature behavior between compounds with different anions, the resistivities in Fig. 2 are normalized to room-temperature values. As can be seen, all three compounds show semiconducting behavior in the entire temperature range, as expected for Mott insulators. The change in resistivity with temperature is most pronounced for κ-B, less for κ-Ag, and least for κ-Cu. The difference between compounds can be quantitatively expressed by comparing the values of the ratio $\rho(T)/\rho_{\mathrm{RT}}$ at certain temperatures. Taking, e.g., 80 K, which is the lowest temperature with the data for all three compounds, $\rho(T)/\rho_{\mathrm{RT}}$ is 40, 200, and 200 000 for κ-Cu, κ-Ag, and κ-B, respectively.

The out-of-plane anisotropy is large and does not change much with temperature (not shown). Expressed as the ratio of the resistivities for the lowest- and the highest-conducting direction, it has the value in the range 100–1000 for κ-Cu [3,4], around 600 for κ-Ag, and around 15 000 for κ-B. The in-plane anisotropy is shown in Fig. 3 as a function of temperature for all three compounds. While for κ-Cu and κ-Ag the in-plane anisotropy $\rho_c/\rho_b \approx 1$ in the temperature interval 50 K $< T <$ 300 K, showing quasi-2D behavior, for κ-B the in-plane anisotropy $\rho_a/\rho_c \approx 6$ in the entire measured temperature range, in accordance with its more pronounced quasi-1D nature found in magnetic measurements and band-structure calculations [25].

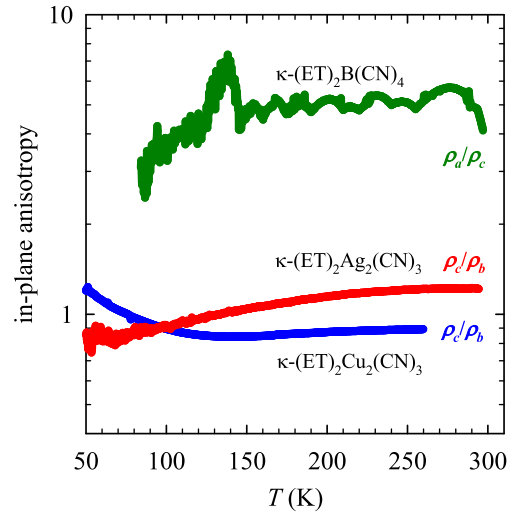

FIG. 3. Temperature dependence of the in-plane anisotropy for κ-Cu (ρ_c/ρ_b, blue line), κ-Ag (ρ_c/ρ_b, red line), and κ-B (ρ_a/ρ_c, green line).

Looking back at Fig. 2 it can be seen that none of the compounds shows simple thermally activated behavior described by a single temperature-independent energy gap E_g in the entire temperature range,

$$\rho \propto \exp(E_g/2T). \tag{2}$$

This is even more obvious in the plot of the logarithmic resistivity derivative $d \ln \rho/d(1/T)$ versus temperature shown in Fig. 4. In the case of the simple activated behavior described by Eq. (2), $d \ln \rho/d(1/T)$ is constant and its value equals half

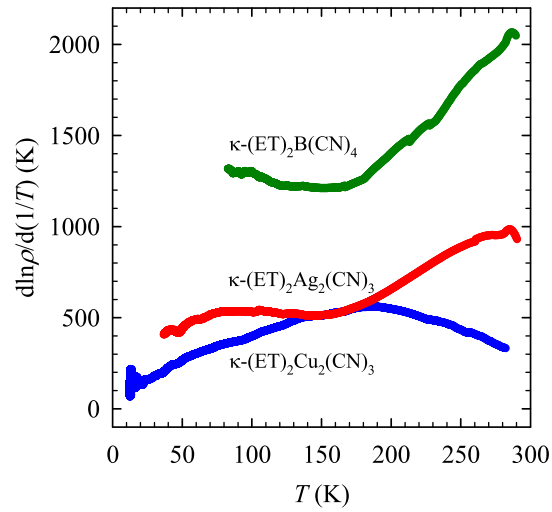

FIG. 4. Temperature dependence of the logarithmic resistivity derivative $d \ln \rho/d(1/T)$ for the highest-conducting direction for κ-Cu (blue line), κ-Ag (red line), and κ-B (green line).

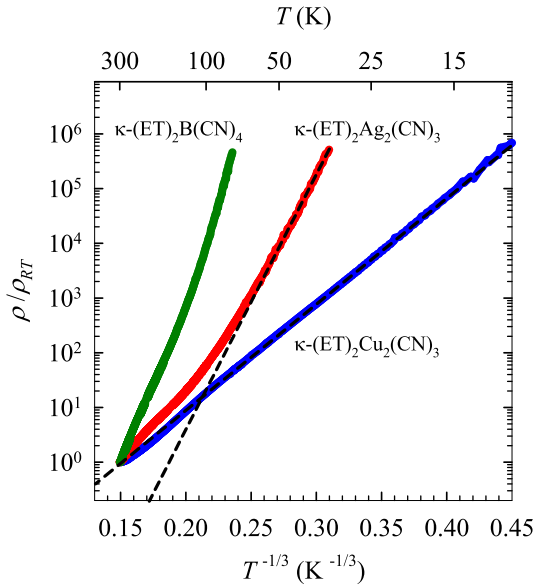

FIG. 5. The normalized resistivity ρ/ρ_{RT} vs $T^{-1/3}$ along the highest-conducting direction for κ-Cu (blue line), κ-Ag (red line), and κ-B (green line). Black dashed lines are fits to 2D VRH (see text).

the energy gap $E_g/2$. As can be seen in Fig. 4, $d \ln \rho/d(1/T)$ in our case shows a pronounced temperature dependence for all three compounds, excluding the presence of a clear transport gap expected for Mott insulators [14].

Our previous dc resistivity and magnetotransport measurements [3,4] on κ-Cu clearly show that at low temperatures charge transport takes place via a Mott 2D VRH mechanism. The same behavior was also mentioned for κ-Ag based on dc resistivity results in a recent publication of our group [24]. The VRH mechanism is typical for disordered systems where electric conduction stems from electron hopping among disorder-induced localized states at the Fermi level and can be described by the expression

$$\rho \propto \exp(T_0/T)^{1/(d+1)}, \tag{3}$$

where T_0 is the characteristic Mott temperature and d is the dimensionality of the system [32]. At higher temperatures VRH can cross over to a nearest-neighbor hopping (NNH), which is a simple thermally activated process described by an equation analogous to (2).

Figure 5 shows the data from Fig. 2 on a log ρ-$T^{-1/3}$ scale suitable for the 2D VRH ($d = 2$). As we can see, while the data for κ-Cu remarkably follow the 2D VRH mechanism, the data for κ-Ag and κ-B are less convincing. Therefore, we decided to follow the procedure outlined in several papers [33–37] where one starts from the more general expression for resistivity,

$$\rho \propto \exp(C/T)^p, \tag{4}$$

and where the exponent p is determined in a self-consistent way. For $C = T_0$ and $p = 1/(d+1)$, Eq. (4) reduces to Eq. (3), and for $C = E_g/2$ and $p = 1$, it reduces to Eq. (2). The procedure is based on a special logarithmic resistivity derivative $X = -d \ln \rho/d \ln T$ which for Eq. (4) gives

$$X = -\frac{d \ln \rho}{d \ln T} = p\left(\frac{C}{T}\right)^p. \tag{5}$$

The exponent p can then be obtained from the slope of $\ln X$ vs $\ln T$.

The $\ln X$ vs $\ln T$ plots are shown in Fig. 6 for all three compounds. In the case of κ-Cu, the slope in the $\ln X$-$\ln T$ graph for $T < 100$ K shows excellent agreement with the value $p = 1/3$ related to 2D VRH and at high temperatures up to ≈200 K it shows good agreement with the value $p = 1$ related to simple activated behavior which is ascribed to NNH. The complex behavior of the slope around 100 K can then be associated with a crossover from 2D VRH to NNH.

In the $\ln X$-$\ln T$ plot for κ-Ag, three different regions can be clearly discerned. There is a wide temperature range between 60 and 180 K where the $\ln X$-$\ln T$ data agree with the value $p = 1$ showing simple activated behavior. This is consistent with a plateau in the logarithmic resistivity derivative $d \ln \rho/d(1/T)$ with the value ≈500 K in the same temperature range shown in Fig. 4. Below 60 K there is a clear change of the slope towards the values of $p < 1$. As can be seen, the data at low temperatures show satisfactory agreement with the value $p = 1/3$ for 2D VRH [24]. The simple activated behavior in the intermediate temperature range can then, as for the κ-Cu compound, be ascribed to the NNH mechanism. At high temperatures $\ln X$ vs $\ln T$ shows complicated behavior which prevents the determination of p. In the same temperature range $d \ln \rho/d(1/T)$ increases with increasing temperature and shows a tendency for saturation around room temperature (see Fig. 4), possibly indicating the activation of charge carriers across an energy gap with the value $E_g/2 \approx 1000$ K. A similar saturation of $d \ln \rho/d(1/T)$ close to room temperature is found also in the transport investigation of κ-Ag under pressure [23]. Such behavior could be ascribed to the presence of some form of mixed conductivity which includes both NNH and activation across the energy gap, as was suggested for semi-insulating GaAs compounds [38] and will be discussed later. The mixed conductivity regime is most probably also present in κ-Cu, which is evident from the deviation of the $\ln X$-$\ln T$ data from the $p = 1$ line in Fig. 6 above 200 K.

Similarly to κ-Ag, κ-B shows a wide temperature interval between 80 and 190 K with a simple activated behavior described by $p = 1$, followed by the complex behavior of the $\ln X$-$\ln T$ at high temperatures. However, the value of $d \ln \rho/d(1/T) \approx 1300$ K estimated from the plateau in Fig. 4 is much higher than for κ-Ag. A crossover from simple activated behavior to VRH at low temperatures, if present at all, could not be detected due to very high resistances below 80 K. Therefore, we performed fits to the 2D VRH mechanism only for κ-Cu and κ-Ag and in the temperature range consistent with the value $p = 1/3$, which is indicated by the black dashed lines in Fig. 5. The values of the Mott temperatures T_0 extracted from the slope of the fits are around 9×10^4 and 7×10^5 K for κ-Cu and κ-Ag, respectively. The $\ln X$-$\ln T$ analysis is practically identical for the other in-plane direction for all three compounds, which is evident from the almost temperature-independent in-plane anisotropy

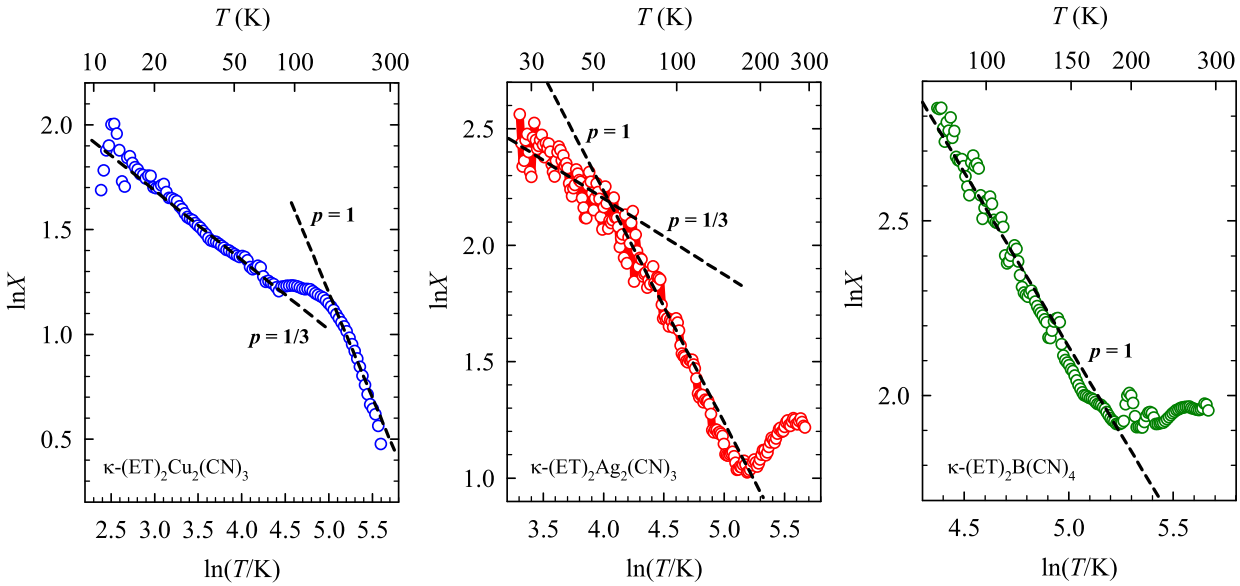

FIG. 6. ln X vs ln T for the highest-conducting direction for κ-Cu (left panel), κ-Ag (middle panel), and κ-B (right panel). Black dashed lines correspond to the slopes expected for the 2D VRH ($p = 1/3$) and simple activated behavior ($p = 1$).

shown in Fig. 3. It is worth mentioning that there is another type of hopping in the literature known as Efros-Shklovskii VRH which is present in disordered systems with strong electron-electron interactions. It is mathematically equivalent to the Mott VRH in one dimension, i.e., $p = 1/2$ and $C = T_0$ in Eq. (4). However, Efros-Shklovskii VRH refers to a 3D system and the meaning of the parameter T_0 is different than in the Mott 1D VRH [39]. Looking at Fig. 6, we can rule out the presence of Efros-Shklovskii VRH in all three compounds in the entire measured temperature range.

We know [3,24] that the hopping conductivity in κ-Cu and κ-Ag can be ascribed to the CN disorder within insulating layers which is transferred to the conducting ET layers via hydrogen bonds between disordered CN groups and ethylene groups, more effectively in κ-Cu than in κ-Ag [3,7,24]. Support for such a scenario can be found in the x-ray diffraction [5] measurements which in the case of κ-Cu indicated an ordering of the ethylene groups in a staggered conformation around 150 K. Looking at Fig. 6, we can see that around the same temperature there is a crossover from 2D VRH to NNH for κ-Cu. In the case of κ-Ag the ethylene groups order already at room temperature [23]. However, ^{1}H-NMR measurements in the same paper [23] found a strong increase in the T_1^{-1} signal above 200 K, which was attributed to the thermal motions of the ethylene groups. Looking at Fig. 6, we can see that around the same temperature there is a crossover from NNH to a mixed conductivity regime for κ-Ag. The relationship between ethylene groups and our hopping transport is in both compounds most easily understood within the scenario of CN disorder being transferred to the conducting ET layers via hydrogen bonds.

In contrast to κ-Cu and κ-Ag, the crystal structure of κ-B does not possess crystallographically disordered CN groups [25]. It is then surprising that the dc resistivity shows a strong deviation from simple activated behavior above 200 K, very similar to the one found in κ-Ag (see Fig. 6). The similarity between κ-B and κ-Ag is even more obvious if we note that the ^{1}H-NMR T_1^{-1} signal of κ-B starts to be governed by thermal motions of the ethylene groups above 200 K, right at the temperature where the deviation is found. This implies the existence of a strong link between the dc transport and the ethylene groups. An increase of $d \ln \rho / d(1/T)$ in the temperature range 200 K $< T <$ 300 K (see Fig. 4) and very likely the appearance of a new plateau above room temperature is by analogy with κ-Ag most easily understood as a crossover from NNH to a mixed conductivity regime (which includes both NNH and activation across the energy gap). Therefore, at least some level of disorder should be present within the insulating $B(CN)_4$ layers. For the source of the disorder, the molecular rotation of $B(CN)_4$ anions may be a possible candidate, although no sign of such dynamic behavior was visible from x-ray diffraction measurements [25]. This proposal remains to be clarified in a future study. It is worth noting that recent dc resistivity and dielectric spectroscopy measurements by our group on κ-$(ET)_2Cu[N(CN)_2]Cl$ [18], which belongs to the same family as the three compounds investigated here and with all CN groups ordered, also pointed towards the presence of disorder within the conducting ET layers, the origin of which for now remains a mystery. Also, a recent magnetotransport study of α-$(ET)_2I_3$ [40], which has a different arrangement of ET molecules, revealed hopping conductivity and negative magnetoresistance at low temperatures that were both ascribed to disorder within insulating I_3 layers which is transferred to the conducting layers via hydrogen bonds. Therefore, it seems likely that the presence of intrinsic disorder is common among the compounds of the ET family.

To summarize, all three compounds which are, according to theory, Mott insulators reveal the presence of disorder and some form of hopping conductivity which takes place upon reducing temperature. κ-Cu has the highest, κ-Ag the intermediate, and κ-B the lowest level of disorder within the conducting ET layers. This seems to be the most important difference between the three compounds, so it should be responsible for the large differences found in our dc transport

data. The most disordered κ-Cu shows at the same time the least insulating behavior, while the least disordered κ-B shows the most insulating behavior. This is at first sight counterintuitive and in contrast with the standard theory of Anderson localization [41] where with increasing disorder electronic states tend to be more localized, i.e., a system becomes more insulating. However, in the more advanced theory of Mott-Anderson localization [20–22] there is a part of the phase diagram where indeed a disorder increase drives the system from an insulating towards a metallic state. Such behavior is argued as follows. When the disorder strength is sufficiently weak, the single-particle correlation gap might survive despite the appearance of disorder-induced localized states within the gap. With increasing disorder, there are more localized states within the gap, which in turn leads to a higher conductivity of a system. This part of the phase diagram appears for an intermediate correlation strength $1 < U/W < 2.5$ [20], which is exactly in the range where the U/W values for our three compounds lie. According to the theory, the most disordered κ-Cu should have the highest carrier density, while the least disordered κ-B should have the lowest carrier density. It is therefore very important to look at the Hall effect data for κ-Cu, κ-Ag, and κ-B which we do in the following section.

The existence of localized states within a correlation gap can easily explain the presence of hopping conductivity found for all three compounds. The mixed conductivity regime close to room temperature can then be viewed as composed of two channels: one channel which describes a part of the charges that hop between localized states within the correlation gap, and the other channel which describes a part of the charges that are thermally activated across the correlation gap. The tendency of saturation of $d\ln\rho/d(1/T)$ around room temperature in κ-Ag (see Fig. 4) indicates that the activation across the correlation gap becomes a dominant conductivity channel for $T > 300$ K. The same scenario is expected in κ-B for even higher temperatures. In contrast to κ-Ag and κ-B, $d\ln\rho/d(1/T)$ for κ-Cu after the first plateau at intermediate temperatures associated with NNH decreases with increasing temperature (see Fig. 4). It is then hard to imagine the appearance of another plateau at high temperatures which would be associated with the activation of charge carriers across the correlation gap.

Recent optical spectroscopy and pressure-dependent dc transport measurements together with dynamical mean-field theory calculations [8] revealed the importance of the quantum Widom line in the phase diagram of frustrated Mott insulators. The quantum Widom line separates the Mott state with a well-defined correlation (Mott-Hubbard) gap and the incoherent conduction regime where the Hubbard bands are strongly blurred by thermal broadening. It is determined as the global maximum in a logarithmic resistivity derivative $d\ln\rho/d(1/T)$ [8]. Looking at Fig. 4, we can see that the global maximum in $d\ln\rho/d(1/T)$ for κ-Cu appears around 200 K, indicating that for $T > 200$ K, κ-Cu enters the incoherent conducting regime, which could explain the absence of an additional plateau at high temperatures which would be associated with the activation of charge carriers across the correlation gap. The logarithmic resistivity derivative $d\ln\rho/d(1/T)$ in the case of κ-Ag shows the global maximum around room temperature (Fig. 4), which implies that the incoherent conduction regime in κ-Ag appears at higher temperatures than in κ-Cu, in accordance with the dc transport results from Ref. [8]. Such behavior is ascribed to the difference in correlation strength U/W which, determined from optical measurements $U/W = 1.52$ for κ-Cu and $U/W = 1.96$ for κ-Ag, indicates that κ-Ag is deeper in the Mott state than κ-Cu [8]. According to Fig. 4, κ-B could enter the incoherent conduction regime well above room temperature, which would imply that it is even deeper in the Mott state. Since the calculated bandwidth W is comparable in the three compounds, 390 meV for κ-B [25], and around 450 meV for κ-Ag and κ-Cu [7,8], the different positions in the phase diagram seem to relate mostly to the Coulomb repulsion U which determines the overall size of the Mott-Hubbard gap. To place κ-B more reliably in the phase diagram, optical spectroscopy results (which enable a direct extraction of the bandwidth W and Coulomb energy U) are highly desirable.

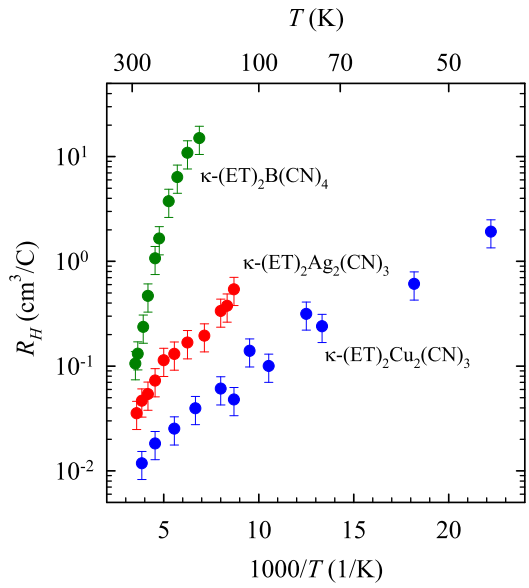

FIG. 7. Temperature dependence of the Hall coefficient R_H for κ-Cu (blue symbols), κ-Ag (red symbols), and κ-B (green symbols).

B. Carrier densities and closeness to the metal-insulator transition

The temperature dependence of the Hall coefficient R_H is shown in Fig. 7. As can be seen, R_H is positive (holelike), and increases with decreasing temperature for all three compounds. The change in $R_H(T)$ is most pronounced for κ-B, less for κ-Ag, and least for κ-Cu, showing similar behavior as the corresponding dc resistivity. This is even more obvious in Fig. 8 where the temperature dependence of R_H and the corresponding dc resistivity are shown on the same plot. As can be seen, the Hall coefficient approximately follows the same temperature dependence as the dc resistivity, which is a common feature of conventional semiconductors. According to theoretical considerations [6,24,25,42], it is expected that only holes contribute to electrical transport in these compounds, and therefore we will use the simplest single-band

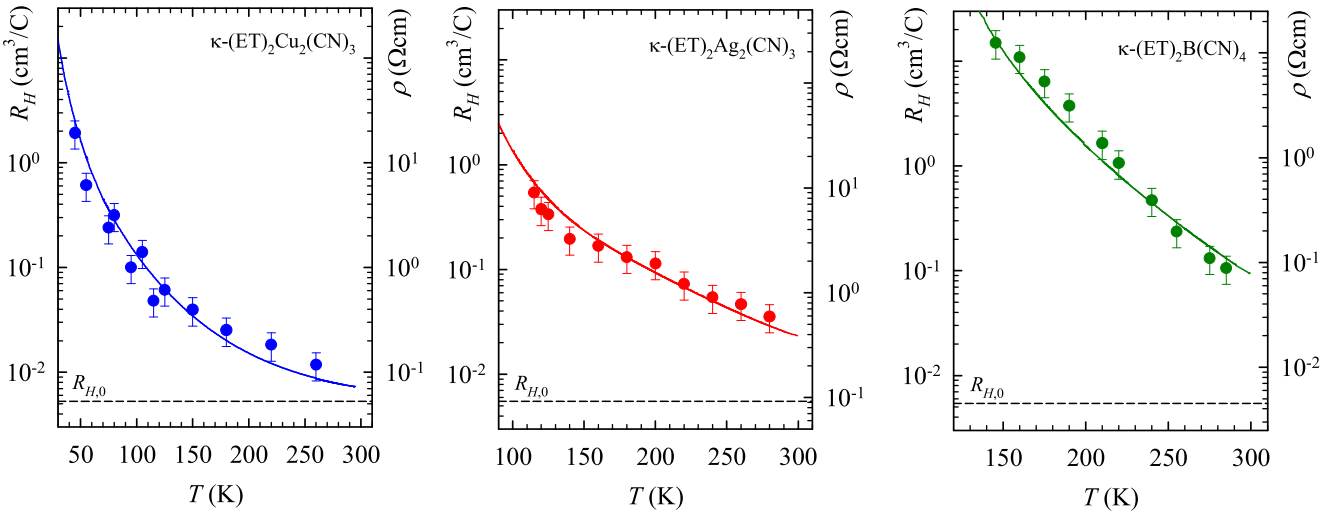

FIG. 8. Temperature dependence of the Hall coefficient R_H (symbols) and resistivity ρ along the highest-conducting direction (lines) for κ-Cu (left panel), κ-Ag (middle panel), and κ-B (right panel). Black dashed lines correspond to the Hall coefficient calculated for a half-filled band $R_{H,0}$ (see text).

theory for resistivity and the Hall coefficient to qualitatively understand such behavior,

$$\rho = \frac{1}{ne\mu}, \tag{6}$$

$$R_H = \frac{1}{ne}, \tag{7}$$

and where n and μ are the density and mobility of free charge carriers, respectively, and e is the electron charge. Since carrier mobilities usually slowly change with temperature in a power-law manner, the temperature dependence of the resistivity and Hall coefficient in semiconductors are almost completely determined by a strong exponential behavior of the carrier densities. It should be noted that Eqs. (6) and (7) are valid only for an isotropic energy band, so they are oversimplified for complex systems such as κ-Cu, κ-Ag, and κ-B. Therefore, we will take Eqs. (6) and (7) only for a qualitative description, and we will talk about the effective charge carrier densities n_{eff} and mobilities μ_{eff} instead of real ones.

A significant difference between the three compounds can be also seen in the values of the Hall coefficients or equivalently in the values of the effective carrier densities. Taking, e.g., the values of R_H near room temperature, we get the effective carrier densities $n_{\text{eff}} = 5.2 \times 10^{20}$, 1.8×10^{20}, and 0.6×10^{20} cm^{-3} for κ-Cu, κ-Ag, and κ-B, respectively. The fact that near room temperature the effective carrier density in κ-Cu is around three times larger than in κ-Ag and almost an order of magnitude larger than in κ-B is in agreement with the corresponding temperature dependence of ρ and R_H. What is more important, the measured n_{eff} is in full accordance with the earlier mentioned theory of Mott-Anderson localization, according to which the highest carrier density in κ-Cu reflects the highest density of disorder-induced localized states around the Fermi level. The effective carrier mobilities μ_{eff} calculated from Eqs. (6) and (7) turned out to be approximately the same (within the error bars) for all three compounds and of the order 0.1 cm^2 V^{-1} s^{-1} around room temperature. The effective mobility is almost independent on temperature (not shown), except for κ-Cu below 100 K where it follows the temperature dependence expected for 2D VRH [4].

A simple charge transfer consideration between organic ET and the inorganic X subsystem leads to 1/2 hole per ET molecule. Taking into account four ET molecules in the unit cell, there are two holes per unit cell for κ-Cu and κ-Ag. In the case of κ-B there are eight ET molecules, i.e., four holes per unit cell. If the corresponding ET bands were degenerate, these bands would be quarter filled by holes. However, ET bands in the κ family are split into upper and lower branches due to the strong dimerization of ET molecules, leading to an effectively half-filled system with holes [6,24,25,42], which implies a metallic state. However, as shown in Fig. 2, all three compounds do not show metal-like behavior in the entire temperature range. Nevertheless, a rough estimate for the carrier density n_0 and Hall coefficient $R_{H,0}$ calculated from stoichiometry can serve as an indication of a proximity or a distance from the metallic state. Taking the unit cell volumes at room temperature, 1695 [5], 1757 [7], and 3487 Å^3 [25] for κ-Cu, κ-Ag, and κ-B, respectively, gives approximately the same value of $R_{H,0} \approx 5 \times 10^{-3}$ cm^3/C for all three compounds, indicated by the black dashed lines in Fig. 8.

As can be seen, in the case of κ-Cu, the measured R_H near room temperature is very close to the value calculated for a half-filled (metallic) band. Comparing the effective carrier density n_{eff} calculated from the measured R_H with the carrier density expected for a half-filled band n_0, we get near room temperature $n_{\text{eff}}/n_0 \approx 50\%$. The fact that the effective carrier density is the same order of magnitude as the carrier density expected for a half-filled band gives by now the strongest confirmation that κ-Cu lies close to the metal-insulator transition. Indeed, metallic and even superconducting behavior in κ-Cu was found under a pressure of only $\approx$4 kbar [43], and metal-like dc resistivity above 200 K was also achieved by x-ray irradiation-induced carrier doping

[44]. In the case of κ-Ag, $n_{\text{eff}}/n_0 \approx 15\%$, and in the case of κ-B, $n_{\text{eff}}/n_0 \approx 5\%$ near room temperature, showing that κ-Ag is farther from the metal-insulator transition than κ-Cu, and κ-B is the farthest. These conclusions are in accordance with the fact that metallic and superconducting behaviors in κ-Ag are induced for pressures >9 kbar [23], and in the case of κ-B even pressures as large as 25 kbar are not enough to suppress the insulating and establish a metallic state [25]. The comparison of the measured charge carrier densities n_{eff} with the ones calculated for a half-filled band n_0 strongly confirms that the most disordered κ-Cu lies closest and the least disordered κ-B farthest from the metal-insulator transition, in accordance with the phase diagram of the Mott-Anderson localization theory. It is worth mentioning that the previous results for κ-Cu [3], where samples from three different batches were explored, are fully consistent with the present scenario. The samples from the batch with the highest disorder showed the least, while the samples from the batch with the lowest disorder showed the most insulating behavior.

The presence of Mott-Anderson localization in κ-Cu, κ-Ag and κ-B emphasizes the importance of disorder which gets more pronounced upon lowering the temperature. This is important because evidence accumulates that the spin-liquid ground state does not originate solely from the geometric frustration but that disorder also plays a decisive role [17–19]. Additional experimental and theoretical studies are needed to estimate disorder strength [45] and to fully understand the role of disorder in this family of compounds, especially in the case of κ-B whose origin of disorder is still unknown.

IV. CONCLUSIONS

Despite high similarities in the chemical compositions and crystal structures between κ-Cu, κ-Ag, and κ-B, large differences in dc resistivity ρ and the Hall coefficient R_H have been found. ρ for all three compounds shows insulating behavior which is most pronounced for κ-B and least for κ-Cu. R_H is positive (holelike) and approximately follows the temperature behavior of the corresponding ρ. R_H near room temperature is in the case of κ-Cu close to the value calculated for a half-filled (metallic) band $R_{H,0}$, indicating that κ-Cu lies close to a metal-insulator transition. R_H for κ-Ag is significantly higher than $R_{H,0}$ and for κ-B is the highest, indicating that κ-Ag is farther and κ-B is the farthest from the metallic state.

In the case of κ-Cu and κ-Ag, three different conductivity regimes were discerned: 2D VRH at low, NNH at intermediate, and a mixed conductivity at high temperatures. Hopping conductivity in κ-Cu and κ-Ag is ascribed to the crystallographic disorder of CN groups which is transferred to the conducting layers via hydrogen bonds, more effectively in κ-Cu than in κ-Ag. In the case of κ-B, the CN groups of which are all ordered, only NNH and the mixed conductivity regime were detected. This implies that some level of disorder should exist also in κ-B but its origin remains an open question for a future study.

The most disordered, κ-Cu, is closest to the metal-insulator transition, while the least disordered, κ-B, is farthest from it. Such counterintuitive behavior can be understood within the Mott-Anderson theory according to which there is a part of the phase diagram where a disorder introduces localized states within a correlation gap, increasing in that way the conductivity, i.e., pushing a system towards the metal-insulator transition. Besides localized, there are also delocalized states which can explain the presence of both a hopping and a mixed conductivity regime. The presence of Mott-Anderson localization emphasizes the importance of disorder in selected materials which is crucial in the formation of their quantum-spin-disordered state. Further work is needed to fully understand such an intricate interplay between correlations and disorder, especially in κ-B where the origin of disorder is yet to be clarified.

ACKNOWLEDGMENTS

We thank A. Pustogow for very helpful discussions. This work was supported by the Croatian Science Foundation Project No. IP-2013-11-1011 and by the Deutsche Forschungsgemeinschaft (DFG) under Grants No. DR228/52-1 and No. DR228/41-1. J.A.S. acknowledges support from the Independent Research and Development program from the NSF while working at the Foundation.

M.Č. and E.T. contributed equally to this work.

[1] T. Ishiguro, K. Yamaji, and G. Saito, *Organic Superconductors*, 2nd ed. (Springer, Berlin, 1998).

[2] B. J. Powell and R. H. McKenzie, Rep. Prog. Phys. **74**, 056501 (2011).

[3] M. Pinterić, M. Čulo, O. Milat, M. Basletić, B. Korin-Hamzić, E. Tafra, A. Hamzić, T. Ivek, T. Peterseim, K. Miyagawa, K. Kanoda, J. A. Schlueter, M. Dressel, and S. Tomić, Phys. Rev. B **90**, 195139 (2014).

[4] M. Čulo, E. Tafra, M. Basletić, S. Tomić, A. Hamzić, B. Korin-Hamzić, M. Dressel, and J. A. Schlueter, Physica B **460**, 208 (2015).

[5] H. O. Jeschke, M. de Souza, R. Valentí, R. S. Manna, M. Lang, and J. A. Schlueter, Phys. Rev. B **85**, 035125 (2012).

[6] H. C. Kandpal, I. Opahle, Y.-Z. Zhang, H. O. Jeschke, and R. Valentí, Phys. Rev. Lett. **103**, 067004 (2009).

[7] T. Hiramatsu, Y. Yoshida, G. Saito, A. Otsuka, H. Yamochi, M. Maesato, Y. Shimizu, H. Ito, Y. Nakamura, H. Kishida, M. Watanabe, and R. Kumai, Bull. Chem. Soc. Jpn. **90**, 1073 (2017).

[8] A. Pustogow, M. Bories, A. Löhle, R. Rösslhuber, E. Zhukova, B. Gorshunov, S. Tomić, J. A. Schlueter, R. Hübner, T. Hiramatsu, Y. Yoshida, G. Saito, R. Kato, T.-H. Lee, V. Dobrosavljević, S. Fratini, and M. Dressel, Nat. Mater. **17**, 773 (2018).

[9] U. Geiser, H. H. Wang, K. D. Carlson, J. M. Williams, H. A. Charlier, J. E. Heindl, G. A. Yaconi, B. J. Love, M. W. Lathrop, J. E. Schirber, D. L. Overmyer, J. Q. Ren, and M.-H. Whangbo, Inorg. Chem. **30**, 2586 (1991).

[10] P. Foury-Leylekian, V. Ilakovac, V. Balédent, P. Fertey, A. Arakcheeva, O. Milat, D. Petermann, G. Guillier, K. Miyagawa, K. Kanoda, P. Alemany, E. Canadell, S. Tomic, and J.-P. Pouget, Crystals **8**, 158 (2018).

[11] Y. Shimizu, K. Miyagawa, K. Kanoda, M. Maesato, and G. Saito, Phys. Rev. Lett. **91**, 107001 (2003).

[12] P. W. Anderson, Mater. Res. Bull. **8**, 153 (1973).
[13] K. Nakamura, Y. Yoshimoto, T. Kosugi, R. Arita, and M. Imada, J. Phys. Soc. Jpn. **78**, 083710 (2009).
[14] M. Imada, A. Fujimori, and Y. Tokura, Rev. Mod. Phys. **70**, 1039 (1998).
[15] S. Elsässer, D. Wu, M. Dressel, and J. A. Schlueter, Phys. Rev. B **86**, 155150 (2012); M. Dressel and A. Pustogow, J. Phys.: Condens. Matter **30**, 203001 (2018).
[16] M. Abdel-Jawad, I. Terasaki, T. Sasaki, N. Yoneyama, N. Kobayashi, Y. Uesu, and C. Hotta, Phys. Rev. B **82**, 125119 (2010).
[17] Y. Qi and S. Sachdev, Phys. Rev. B **77**, 165112 (2008).
[18] M. Pinterić, D. Rivas Góngora, Ž. Rapljenović, T. Ivek, M. Čulo, B. Korin-Hamzić, O. Milat, B. Gumhalter, P. Lazić, M. Sanz Alonso, W. Li, A. Pustogow, G. G. Lesseux, M. Dressel, and S. Tomić, Crystals **8**, 190 (2018).
[19] Y. Saito, T. Minamidate, A. Kawamoto, N. Matsunaga, and K. Nomura, Phys. Rev. B **98**, 205141 (2018).
[20] K. Byczuk, W. Hofstetter, and D. Vollhardt, Phys. Rev. Lett. **94**, 056404 (2005).
[21] M. C. O. Aguiar, V. Dobrosavljević, E. Abrahams, and G. Kotliar, Phys. Rev. Lett. **102**, 156402 (2009).
[22] H. Shinaoka and M. Imada, J. Phys. Soc. Jpn. **78**, 094708 (2009).
[23] Y. Shimizu, T. Hiramatsu, M. Maesato, A. Otsuka, H. Yamochi, A. Ono, M. Itoh, M. Yoshida, M. Takigawa, Y. Yoshida, and G. Saito, Phys. Rev. Lett. **117**, 107203 (2016).
[24] M. Pinterić, P. Lazić, A. Pustogow, T. Ivek, M. Kuveždić, O. Milat, B. Gumhalter, M. Basletić, M. Čulo, B. Korin-Hamzić, A. Löhle, R. Hübner, M. Sanz Alonso, T. Hiramatsu, Y. Yoshida, G. Saito, M. Dressel, and S. Tomić, Phys. Rev. B **94**, 161105(R) (2016).
[25] Y. Yoshida, H. Ito, M. Maesato, Y. Shimizu, H. Hayama, T. Hiramatsu, Y. Nakamura, H. Kishida, T. Koretsune, C. Hotta, and G. Saito, Nat. Phys. **11**, 679 (2015).
[26] H. Morita, S. Watanabe, and M. Imada, J. Phys. Soc. Jpn. **71**, 2109 (2002).
[27] B. Kyung and A.-M. S. Tremblay, Phys. Rev. Lett. **97**, 046402 (2006).
[28] H. C. Montgomery, J. Appl. Phys. **42**, 2971 (1971).
[29] E. Tafra, M. Čulo, M. Basletić, B. Korin-Hamzić, A. Hamzić, and C. S. Jacobsen, J. Phys.: Condens. Matter **24**, 045602 (2012).
[30] N. Harrison, M. M. Honold, M. V. Kartsovnik, J. Singleton, S. T. Hannahs, D. G. Rickel, and N. D. Kushch, Phys. Rev. B. **55**, R16005 (1997).
[31] L. I. Buravov, N. D. Kushch, V. N. Laukhin, A. G. Khomenko, E. B. Yagubskii, M. V. Kartsovnik, A. E. Kovalev, L. P. Rozenberg, R. P. Shibaeva, M. A. Tanatar, V. S. Yefanov, V. V. Dyakin, and V. A. Bondarenko, J. Phys. I **4**, 441 (1994).
[32] N. F. Mott and E. A. Davis, *Electronic Processes in Non-Crystalline Solids* (Oxford University Press, London, 1971).
[33] D. Joung and S. I. Khondaker, Phys. Rev. B **86**, 235423 (2012).
[34] S. I. Khondaker, I. S. Shlimak, J. T. Nicholls, M. Pepper, and D. A. Ritchie, Phys. Rev. B **59**, 4580 (1999).
[35] S. I. Khondaker, I. S. Shlimak, J. T. Nicholls, M. Pepper, and D. A. Ritchie, Solid State Commun. **109**, 751 (1999).
[36] C. Chuang, R. K. Puddy, H.-D. Lin, S.-T. Lo, T. M. Chen, C. G. Smith, and C. T. Liang, Solid State Commun. **152**, 905 (2012).
[37] A. G. Zabrodskii, Philos. Mag. B **81**, 1131 (2001).
[38] R. M Rubinger, G. M. Ribeiro, A. G. de Oliveira, H. A. Albuquerque, R. L. da Silva, C. P. L. Rubinger, W. N. Rodrigues, and M. V. B. Moreira, Semicond. Sci. Technol. **21**, 1681 (2006).
[39] A. L. Efros and B. I. Shklovskii, J. Phys. C: Solid State Phys. **8**, L49 (1975).
[40] T. Ivek, M. Čulo, M. Kuveždić, E. Tutiš, M. Basletić, B. Mihaljević, E. Tafra, S. Tomić, A. Löhle, M. Dressel, D. Schweitzer, and B. Korin-Hamzić, Phys. Rev. B **96**, 075141 (2017).
[41] P. W. Anderson, Phys. Rev. **109**, 1492 (1958).
[42] H. Seo, C. Hotta, and H. Fukuyama, Chem. Rev. **104**, 5005 (2004).
[43] Y. Kurosaki, Y. Shimizu, K. Miyagawa, K. Kanoda, and G. Saito, Phys. Rev. Lett. **95**, 177001 (2005).
[44] T. Sasaki, H. Oizumi, N. Yoneyama, N. Kobayashi, and N. Toyota, J. Phys. Soc. Jpn. **76**, 123701 (2007).
[45] K. Gregor and O. I. Motrunich, Phys. Rev. B **79**, 024421 (2009).